Rhinology

Computational fluid dynamics: a suitable assessment tool for demonstrating the antiobstructive effect of drugs in the therapy of allergic rhinitis

La dinamica computerizzata dei fluidi: uno strumento valido per la dimostrazione dell'efficacia dei farmaci sull'ostruzione respiratoria nasale nella terapia della rinite allergica

N. ACHILLES[1], N. PASCH[2], A. LINTERMANN[3], W. SCHRÖDER[3], R. MÖSGES[1]

[1] Institute of Medical Statistics, Informatics and Epidemiology (IMSIE), University Hospital of Cologne, Germany; [2] Otolaryngologist Practice, Aachen, Germany; [3] Institute of Aerodynamics, RWTH Aachen, Germany

SUMMARY

This systematic review aims first to summarize the previous areas of application of computational fluid dynamics (CFD) and then to demonstrate that CFD is also a suitable instrument for generating three-dimensional images that depict drug effects on nasal mucosa. Special emphasis is placed on the three-dimensional visualization of the antiobstructive effect of nasal steroids and antihistamines in the treatment of allergic rhinitis. In the beginning, CFD technology was only used to demonstrate physiological and pathophysiological airflow conditions in the nose and to aid in preoperative planning and postoperative monitoring of surgical outcome in the field of rhinosurgery. The first studies using CFD examined nasal respiratory physiology, important functions of the nose, such as conditioning and warming of inspired air, and the influence of pathophysiological changes on nasal breathing. Also, postoperative outcome of surgical procedures could be "predicted" using the nasal airflow model. Later studies focused on the three-dimensional visualization of the effect of nasal sprays in healthy subjects and postoperative patients. A completely new approach, however, was the use of CFD in the area of allergic rhinitis and the treatment of its cardinal symptom of nasal obstruction. In two clinical trials, a suitable patient with a positive history of allergic rhinitis was enrolled during a symptom-free period after the pollen season. The patient developed typical allergic rhinitis symptoms after provocation with birch pollen. The 3-D visualization showed that the antiallergic treatment successfully counteracted the effects of nasal allergen provocation on nasal airflow. These observations were attributed to the antiobstructive effect of a nasal steroid (mometasone furoate) and a systemic antihistamine (levocetirizine), respectively. CFD therefore constitutes a non-invasive, precise, reliable and objective examination procedure for generating three-dimensional images that depict the effects of drugs used in the treatment of allergic rhinitis.

KEY WORDS: Computational fluid dynamics (CFD) • Nasal airflow simulation • Allergic rhinitis • Nasal obstruction • Nasal steroid • Mometasone furoate nasal spray (MFNS) • Antihistamine • Levocetirizine

RIASSUNTO

Il primo obiettivo della presente review sistematica è quello di un'esposizione concisa delle precedenti aree di applicazione della fluidodinamica computazionale (CFD), ed in seconda istanza dimostrare la validità della metodica nella realizzazione di immagini tridimensionali che mostrino gli effetti dei farmaci sulla mucosa nasale. Inoltre viene accuratamente descritta la possibilità di visualizzare in tre dimensioni l'effetto decongestionante degli steroidi nasali e degli antistaminici nella terapia della rinite allergica. Agli albori dello sviluppo della metodica la CFD veniva unicamente usata sia per dimostrare condizioni fisiologiche e fisiopatologiche di flusso aereo nasale, sia come supporto nel planning pre-operatorio e nel controllo postoperatorio degli esiti della rino-chirurgia. I primi studi che hanno visto l'applicazione della CFD si sono concentrati sullo studio della fisiologia respiratoria, delle funzioni fondamentali del naso come l'umidificazione e il riscaldamento dell'aria inspirata, e dell'influenza delle modifiche fisiopatologiche sulla respirazione nasale. È stata studiata anche la possibilità di utilizzare modelli di flusso aereo nasale per predire l'efficacia di un eventuale chirurgia nasale. Lavori successivi si sono concentrati sulla visualizzazione in tre dimensioni degli effetti topici degli spray nasali in soggetti sani e in soggetti operati. L'utilizzo della CFD nel campo della rinite allergica ha rappresentato un approccio completamente nuovo alla problematica del trattamento dell'ostruzione respiratoria nasale. In due diversi trial clinici sono stati inclusi soggetti con storia clinica di rinite allergica in fase non sintomatica. I pazienti selezionati sono stati quindi sottoposti a provocazione nasale mediante polline di betullacee con l'intento di evocare la sintomatologia allergica. Il rendering 3-D effettuato dopo trattamento farmacologico ha mostrato una riduzione degli effetti della provocazione allergica sul flusso aereo nasale. Queste osservazioni sono state infine attribuite agli effetti decongestionanti rispettivamente dello steroide topico (monetasone furoato) e dell'antistaminico sistemico (levocetirizina) utilizzati. In conclusione la CFD rappresenta un esame non invasivo, preciso, affidabile ed obiettivo, capace di realizzare immagini in tre dimensioni che mostrano gli effetti dei farmaci utilizzati nella rinite allergica.

PAROLE CHIAVE: *Fluidodinamica computazionale (CFD) • Simulazione del flusso aereo nasale • Rinite allergica • Ostruzione nasale • Steroidi topici • Mometasone furoato spray nasale, (MFNS) • Antistaminico • Levocetirizina*

Introduction

Allergic rhinitis (AR) is clinically defined as a "symptomatic disorder of the nose induced by an IgE-mediated inflammation after allergen exposure of the membranes lining the nose" [1 2]. Worldwide, the prevalence of this disease varies from 1 to 40 % [1]. The classic symptoms of AR are nasal obstruction, rhinorrhoea, sneezing and itching in the nose 1. Subjects attempt to prevent AR symptoms as much as possible by avoiding allergens and taking medication (e.g., intranasal corticosteroids, systemic antihistamines) [3-5], as AR poses great restrictions on quality of life. The cardinal symptom of persistent AR is nasal obstruction. It can be assessed via nasal endoscopy, rhinomanometry, acoustic rhinometry and by employing visual analogue scales and patient questionnaires [6].

Among these procedures, rhinomanometry and acoustic rhinometry are established objective test procedures for evaluating nasal patency. In the course of rhinomanometric examination, transnasal pressure and nasal airflow are measured during the breathing cycle, i.e., inspiration and expiration [7]. In contrast, acoustic rhinometry depicts the geometry of the nasal cavity on the basis of reflected ultrasonic waves. By measuring the minimal cross-sectional areas, a computer-aided calculation can then be performed for the volume of one side of the main nasal cavity [8].

These traditional measuring procedures, however, show weaknesses and disadvantages. One such example, described by Clarke et al. [9] and Baraniuk [10], is the minor or partly lacking correlation between subjective symptoms experienced by patients and objectively measured symptoms. Furthermore, correlation among the results from rhinomanometry, acoustic rhinometry and subjective test procedures (nasal sum symptom score, visual analogue scale) does not always prove to be reliable [11 12].

The need for more precise techniques has encouraged the use of computational fluid dynamics (CFD), a mature technology employed widely in engineering to solve and analyze problems that involve fluid flows[13]. The mathematical predictions made via CFD can also be applied to nasal airflow. For the numerical simulation of nasal airflow, patients must undergo nasal computer tomography (CT) or magnetic resonance imaging (MRI) scans [14].

Many of the first flow simulation studies focused on nasal airflow biophysics [15-17.] CFD has already been used for the flow analysis of pathological cases [18-27] and has been proposed as a tool for predicting actual surgical outcomes using a virtual nasal surgery model [28-32]. A new area of application in which CFD technology has been employed successfully is the three-dimensional visualisation of the effect of medications applied intranasally to the nasal mucosa [33-36].

The first aim of this systematic review is to summarize the previous fields of application of CFD (demonstration of physiological and pathophysiological airflow conditions in the nose, preoperative planning, and postoperative monitoring of surgical outcome in the field of rhinosurgery), while the second is to demonstrate that CFD also represents a suitable instrument for modelling drug effects on the nasal mucosa in three dimensions. Special emphasis is placed on the three-dimensional visualisation of the antiobstructive effect of nasal steroids and antihistamines in the treatment of AR.

Previous fields of application of computational fluid dynamics

The applications of CFD were previously limited to the demonstration of physiological and pathophysiological airflow conditions in the nose and to preoperative planning and postoperative monitoring of surgical outcome in the field of rhinosurgery.

Demonstration of physiological and pathological airflow conditions in the nose

A suitable example of the three-dimensional visualisation of the physiological airflow conditions in the nose is the study by Ishikawa et al. published in 2006. The authors investigated differences between inspiratory and expiratory nasal airflow based on CT images. They concluded that during the inspiratory phase, nasal airflow and its degree of turbulence in the middle meatus were much more prominent than in the expiratory phase [15]. Tan et al. observed comparable nasal airflow behaviour in a clinical trial. In the inspiratory phase, turbulence occurred particularly in the anterior part and at the bottom of the nasal cavity. During the expiratory phase, however, no turbulence was measured. The maximum nasal velocity was measured around the plane of palatine velum during both inspiratory and expiratory phases [16]. Wen et al. also examined the physiological airflow conditions in the nose, and observed high velocities in the constrictive nasal valve area region as well as high flow close to the septum walls [17].

In addition, pathophysiological alterations in the nose such as septal deviation [18 21 25 26], turbinate hypertrophy [19 22 24], nasal bone fracture [20], septal perforation [23], deviation of the external nose [27] and their implications can be visualized by CFD technology.

In the controlled clinical trial by Sun et al., for example, patients with nasal septum deviations were compared to subjects with no anatomical changes. Sun et al. concluded that by using nasal airflow simulation, it is possible to visualize the changes in nasal airflow caused by abnormal anatomy of the nose [26]. Liu likewise demonstrated the impact of various forms of septal deviation on nasal airflow characteristics [25.] Similarly, Guo showed that the unilateral hypertrophy infraturbinal also changed normal anatomy and influenced aerodynamics of the nasal cavity. According to Guo, these changes can have a verifiable effect on important functions of the nose such as humidification and warming of respiratory air, in addition to olfaction [22].

In a clinical study in five healthy subjects and using air-

flow simulations based on CT images, Bailie et al. confirmed that the inferior and middle turbinates play a major role in the conditioning (warming up and cooling down) of inspired air. Furthermore, this airflow model might help to explain how wall shear stress occurring along the inferior and middle turbinates can cause epistaxis in Little's area [37]. This clinical study thus substantiated the study results observed by Pless et al. in 2004, who concluded that the inferior and middle turbinates both play a predominant role in heat recovery during the expiratory phase. Furthermore, they observed that the areas with the greatest decrease in temperature were characterised by turbulent airflow [38]. Likewise, Sommer et al. attached substantial importance to the middle turbinate in the conditioning and humidification of inhaled air [39].

In their investigation, Ishikawa et al. addressed olfaction as one of the important functions of the nose. In a three-dimensional airflow model, it was demonstrated that inspired air passed through a wider olfactory area compared to expired air. The sniffing flow, however, passed through the widest olfactory area, with no increase of velocity being observed in the airflow model. They therefore concluded that a recirculating flow strongly promotes olfactory function in the nose [40].

Preoperative planning and postoperative monitoring of surgical outcome in the field of rhinosurgery

Another emphasis of CFD is the preoperative planning and postoperative monitoring of surgical outcome in the field of rhinosurgery. As early as 2000, Bockholt et al. investigated the possible benefit of using nasal airflow simulations in the area of rhinosurgery. They concluded that a preoperative, three-dimensional model of the nasal cavity based on CT scans can optimize surgical planning and thereby markedly improve the success of surgery [28]. In the clinical study by Xiong et al., CFD was likewise tested in the preoperative planning phase and during postoperative monitoring of surgical outcome. The postoperative outcome of patients could be simulated by visualizing nasal airflow before and after a virtual endoscopic procedure [32]. Other research groups also confirmed the suitability of CFD for generating models that show both surgeons and patients the postoperative benefit of surgical procedures (rapid maxillary expansion [29], turbinate surgery of hypertrophic turbinate [19 41], septoplasty and partial lateral turbinectomy [30]).

A further example of the use of CFD technology can be found in the clinical picture of obstructive sleep apnoea syndrome. Airflow simulations were conducted in 2006 by Sung and Xu to obtain better understanding of the pathophysiology of obstructive sleep apnoea syndrome in children and adults [42 43]. Bimaxillary surgery (maxillomandibular advancement) for enlarging the velo-oro-hypopharyngeal airway constitutes the standardized surgical procedure in the treatment of obstructive sleep apnoea syndrome [44]. In a clinical trial by Yu et al. involving two patients with sleep apnoea syndrome, three-dimensional nasal airflow was calculated based on CT images made before and after surgery (maxillomandibular advancement). Postoperatively, CFD showed an enlargement of the upper airway with balanced velocity and pressure conditions. The postoperative clinical results of patients (less breathing effort accompanied by better ventilation) confirmed the predicted surgical outcome [45].

New fields of application of computational fluid dynamics

A new area of application of CFD is the visualization of drug effects on the nasal mucosa via three-dimensional airflow simulations. In a clinical study, Garlapti's group investigated the effectiveness of nasal sprays applied to nasal mucosa. Based on MRI, it was demonstrated that intranasal medications such as nasal sprays are most effective when the patient actively inhales during application. Contrary to expectations, the position of the head had no decisive effect on the distribution of the inhaled aerosol [36]. Frank et al. added to this observation in that they acknowledged that head position affected the deposition of the applied nasal spray only in cases of low or absent inspiratory airflow [34].

Chen et al. also examined the effect of nasal sprays via CFD technology. In the nasal airflow model of their Chinese patient, it became evident that after functional endoscopic sinus surgery (FESS), moderate inspiratory airflow and a particle diameter of approximately 10^{-5}m improves the deposition of nasally applied drugs considerably [33]. Frank et al. concurred with the observations made by Chen et al. Surgical correction of nasal anatomic deformities (example.g. nasal septum deviation) was able to improve drug delivery on the nasal mucosa [34 35].

3-D visualization of the antiobstructive effect of drugs in therapy of allergic rhinitis

The application of CFD technology is not only restricted to the visualization of drug effects in healthy subjects [36] or patients who have already undergone surgery [34 35], but it can also be used in patients who suffer from the symptoms of AR.

The two clinical studies by Mösges et al. described below, it was shown that nasal airflow simulation can also be used in the treatment of AR. The aim of these trials was to verify the antiobstructive effect of a nasal steroid (mometasone furoate nasal spray, MFNS) and a systemic antihistamine (levocetirizine) on the degree to which the nasal mucosa swells under allergen exposure in a three-dimensional nasal airflow model.

These clinical trials were conducted as monocentre, one-arm, prospective, phase IV therapy studies involving the same patient. This 37-year-old female had a positive history of AR (confirmed by skin prick test and nasal provocation test) and was enrolled in the clinical trials during a symptom-free period after the pollen season. She developed typical AR symptoms (especially nasal obstruction) after provocation with birch pollen.

The design of both clinical trials was nearly identical and is summarized in Table I. The trials differed from each other only in length: MFNS was administered for 14 study days and levocetirizine for 35 days. This differing study period appeared to make sense in view of preliminary studies by Bachert, Canonica, and De Vos on the antiobstructive effect of levocetirizine [46-48].

T2-weighted MRI was used to visualize detailed internal structures and restricted body functions. It provided a three-dimensional image of the nasal cavity, sinuses and pharynx, and allowed the assessment of nasal mucosal swelling. To perform a fluid mechanical analysis of the flow in the human nasal cavity, the surface of the region of interest, i.e., the volume of the nasal cavity, was extracted from MRI data and processed in multiple steps [49]. Since MRI measures the fluid characteristics of different tissues, the distinction between bone and air is generally difficult because they contain no or only a small amount of fluid and give a similar MRI signal, i.e. these areas appear black. To allow a better interface detection, blurring was reduced by sharpening the image, by applying a 3 x 3 x 3 convolution matrix filter, which emphasised the voxel differences depending on the 3 x 3 x 3 neighbourhood around the centre voxel. This supported the manual segmentation of the nasal cavity by an experienced ENT specialist who examined each slice of the three-dimensional image and identified the region of interest (ROI) with a digital pen tablet. The image was then further pre-processed at the Institute of Aerodynamics of RWTH Aachen University. A seeded region growing algorithm [50] was used to identify the previously detected ROI by placing seed points inside the fluid volume of the nasal cavity and recursively descending in the neighbourhood of them. The identification was based on a lower and an upper threshold depending on the assignment method used by the ENT specialist. Based on this segmentation, the marching cubes algorithm [51] was used to extract the surface of the nasal cavity yielding a three-dimensional triangle representation. This algorithm is based on an intensity detection along voxel edges and defines vertices along these lines by a bi-linear interpolation between the intensities at the corners of the voxels. A set of triangles was defined for such a vertex configuration, taken from a configuration table containing 256 possible combinations. In a post-processing step, the surface was smoothed using a windowed sinc function [52], removing high frequency noise in the Fourier space by applying a transfer function. In a final step, the surface was split into multiple parts. The nostrils and the throat were separated from the rest of the nasal cavity and were smoothed with a Laplace filter until convergence. This filter relaxes the mesh and iteratively moves all vertices into one plane. This step allowed the proper application of the boundary conditions in the flow simulation. Based on this model, an automatic Cartesian grid generator created the computational mesh. A minimal bounding cube was initially placed around the surface. This cube was then continuously split into eight smaller cubes until a user-defined level of refinement was reached. During the splitting process, cells outside the fluid domain were removed. The simulation was carried out using a Lattice Boltzmann method and was performed on grids containing about 20 x 10^6 cells. As for the imposed boundary conditions, a no-slip wall condition proposed by Bouzidi et al. [53] was used. A volume flux of 125 ml/sec was prescribed at the inflow boundaries with a von Neumann condition for the velocity. The density was extrapolated in surface normal direction by applying a Dirichlet condition. The outflow boundary condition was based on the formulation by Finck et al. [54] and imposed a constant pressure and extrapolated the velocities. The Reynolds number, based on the mean hydraulic diameter of the nostrils and a volume flux of 125 ml/sec, was calculated for all nasal cavity geometries to guarantee an equal volume flux in all cases.

Table I. Study design.

	Treatment period			
	Visit 1	Visit 2	Visit 3	Visit 4
Written consent	X			
Collection of demographic data	X			
Assessment of inclusion and exclusion criteria	X			
Medical history	X			
Physical examination	X	X	X	X
Examination by ENT specialist	X	X	X	X
Nasal endoscopy	X	X	X	X
Rhinomanometry	X	X	X	X
Acoustic rhinometry	X	X	X	X
MRI examination		X		X
Nasal provocation test	X	X	X	X
Rhinomanometry	X	X	X	X
Acoustic rhinometry	X	X	X	X
MRI examination		X		X

The results of nasal airflow simulation for the MFNS study are depicted in Figures 1 and 2. Figure 1 shows the direct comparison between airflow conditions in the nasal cavity without MFNS use before and after allergen provocation. Prior to allergen provocation, two opened airflow channels were visible at the entrance to the nose and the flow velocity was high. After nasal provocation testing, however, only one airflow channel was visible and the flow velocity was considerably reduced. This observation is consistent with a marked swelling of the nasal mucosa, triggered by exposure to birch pollen.

Figure 2 shows the comparison of the nasal flow conditions under MFNS use before and after allergen provocation. Following a 14-day application of MFNS, three airflow channels were clearly discernible prior to allergen provocation. After provocation with birch pollen, the nasal volume flow was in fact reduced, but the decrease was considerably smaller.

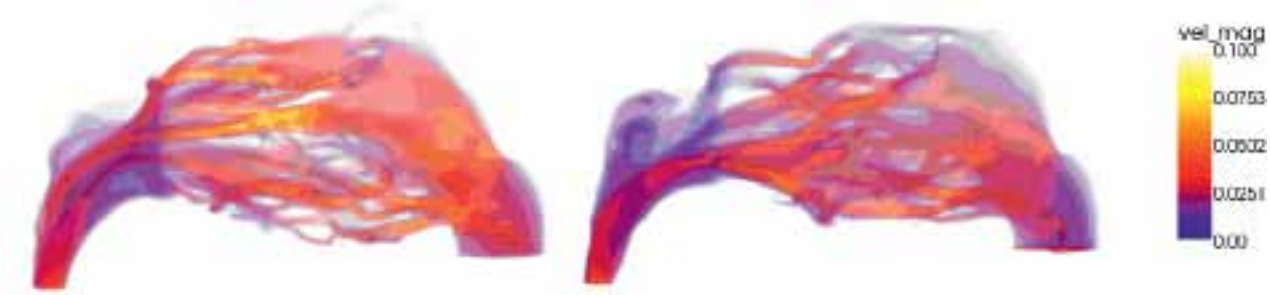

Fig. 1. Nasal airflow without MFNS use before (left) and after (right) allergen provocation.

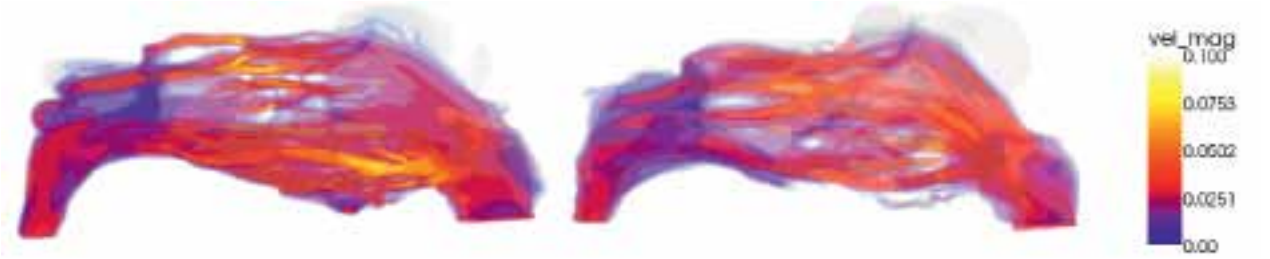

Fig. 2. Nasal airflow under MFNS use before (left) and after (right) allergen provocation.

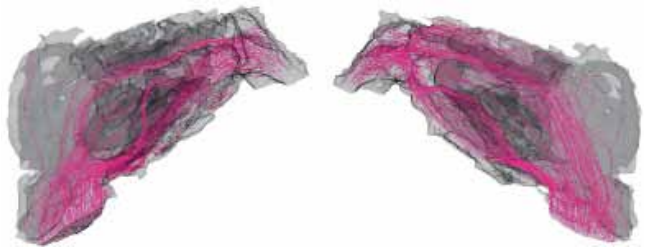

Fig. 3. Streamlines (Visit 2 before allergen provocation).

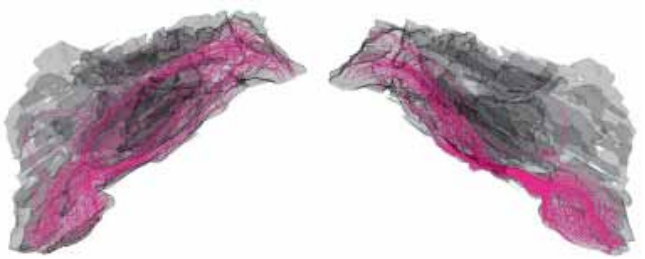

Fig. 4. Streamlines (Visit 2 after allergen provocation).

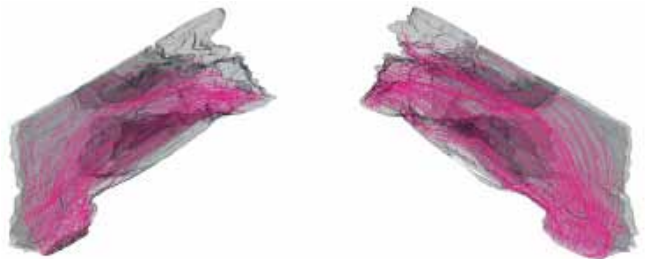

Fig. 5. Streamlines (Visit 4 before allergen provocation).

Fig. 6. Streamlines (Visit 4 after allergen provocation).

It therefore became apparent that the antiobstructive effect of MFNS on the degree of swelling of the nasal mucosa, already demonstrated in numerous studies [55-57], could also be verified through nasal airflow simulation [58].

The streamlines in Figures 3-6 provide information about the distribution of nasal airflow before and after allergen provocation during 35-day treatment with levocetirizine. The streamlines originate from the left (left image) and right (right image) nostrils, respectively, and proceed toward the pharynx.

In particular, it became evident that in the nasal geometry from Visit 2 a considerably larger volume flowed through the middle airflow channel before allergen provocation than was the case after provocation. When comparing the streamlines with those from Visit 4, this difference was hardly discernible. In both cases, air flowed through both the lower and the middle airflow channels. The difference between the streamlines showed that by using nasal airflow simulation, a reaction of the nasal mucosa in the form of obstruction could be demonstrated following allergen provocation. Furthermore, nasal obstruction diminished over the entire study period of 36 days. Therefore, the antiobstructive effect of levocetirizine on the degree of nasal mucosal swelling, as

previously described in the medical literature [59-61], could be clearly verified by nasal airflow simulation.

Conclusions

Leong et al. have already recognised the potential of CFD technology in a systematic overview [13]. The present study confirms the results by Leong et al. in 2010. Up to now, nasal airflow simulation served to demonstrate the physiological and pathological airflow conditions in the nose as well as aid in preoperative planning und postoperative monitoring of surgery outcome in rhinosurgery. Previous medical literature likewise shows that nasal airflow simulation can also be used successfully in obstructive sleep apnoea syndrome.

A new development, however, is the visualization of drug effects on the nasal mucosa via CFD technology. In the beginning, its application was limited to the three-dimensional visualization of the effect of intranasally applied sprays in healthy or postoperative patients. The present review shows that nasal airflow simulation can also be employed effectively in the field of AR and in treatment of its cardinal symptom of nasal obstruction. The two aforementioned clinical studies by Mösges et al. demonstrated the antiobstructive effect of both a nasal steroid (MFNS) and a systemic antihistamine (levocetirizine) on the degree of nasal mucosal swelling in a nasal airflow model. Therefore, CFD constitutes a suitable tool for the three-dimensional visualization of drug effects in the therapy of AR.

References

1. Bousquet J, Van Cauwenberge P, Khaltaev N. *Allergic rhinitis and its impact on asthma.* J Allergy Clin Immunol 2001;108(5 Suppl):S147-334.
2. Bachert C, Borchard U, Wedi B, et al. *Allergic rhinoconjunctivitis. Guidelines of the DGAI in association with the DDG.* J Dtsch Dermatol Ges 2006;4:264-75.
3. Meltzer EO, Caballero F, Fromer LM, et al. *Treatment of congestion in upper respiratory diseases.* Int J Gen Med 2010;3:69-91.
4. Prenner BM, Schenkel E. *Allergic rhinitis: treatment based on patient profiles.* Am J Med 2006;119:230-7.
5. Shedden A. *Impact of nasal congestion on quality of life and work productivity in allergic rhinitis: findings from a large online survey.* Treat Respir Med 2005;4:439-46.
6. Wheeler SM, Corey JP. *Evaluation of upper airway obstruction - an ENT perspective.* Pulm Pharmacol Ther 2008;21:433-41.
7. Vogt K, Jalowayski A A, Althaus W, et al. *4-Phase-Rhinomanometry (4PR) - basics and practice 2010.* Rhinol Suppl 2010;(21):1-50.
8. Clement PA, Gordts F. *Consensus report on acoustic rhinometry and rhinomanometry.* Rhinology 2005;43:169-79.
9. Clarke JD, Hopkins ML, Eccles R. *Evidence for correlation of objective and subjective measures of nasal airflow in patients with common cold.* Clin Otolaryngol 2005;30:35-8.
10. Baraniuk JN. *Subjective nasal fullness and objective congestion.* Proc Am Thorac Soc 2011;8:62-9.
11. Andre RF, Vuyk HD, Ahmed A, et al. *Correlation between subjective and objective evaluation of the nasal airway. A systematic review of the highest level of evidence.* Clin Otolaryngol 2009;34:518-25.
12. Haavisto LE, J I S. *Acoustic rhinometry, rhinomanometry and visual analogue scale before and after septal surgery; a prospective ten-year follow up*. Clinical Otolaryngology [Original Manuscript] 2012; 03.11.2012:[Available from: http://onlinelibrary.wiley.com/doi/10.1111/coa.12043/pdf.
13. Leong SC, Chen XB, Lee HP, et al. *A review of the implications of computational fluid dynamic studies on nasal airflow and physiology.* Rhinology 2010;48:139-45.
14. Bailie N, Hanna B, Watterson J, et al. *An overview of numerical modelling of nasal airflow.* Rhinology 2006;44:53-7.
15. Ishikawa S, Nakayama T, Watanabe M, et al. *Visualization of flow resistance in physiological nasal respiration: analysis of velocity and vorticities using numerical simulation.* Arch Otolaryngol Head Neck Surg 2006;132:1203-9.
16. Tan J, Han D, Wang J, et al. *Numerical simulation of normal nasal cavity airflow in Chinese adult: a computational flow dynamics model.* Eur Arch Otorhinolaryngol 2012;269:881-9.
17. Wen J, Inthavong K, Tu J, et al. *Numerical simulations for detailed airflow dynamics in a human nasal cavity.* Respir Physiol Neurobiol 2008;161:125-35.
18. Chen XB, Lee HP, Chong VF, et al. *Assessment of septal deviation effects on nasal air flow: a computational fluid dynamics model.* Laryngoscope 2009;119:1730-6.
19. Chen XB, Lee HP, Chong VF, et al. *Impact of inferior turbinate hypertrophy on the aerodynamic pattern and physiological functions of the turbulent airflow - a CFD simulation model.* Rhinology 2010;48:163-8.
20. Chen XB, Lee HP, Chong VF et al. *Assessments of nasal bone fracture effects on nasal airflow: a computational fluid dynamics study.* Am J Rhinol Allergy 2011;25:e39-43.
21. Garcia GJ, Rhee JS, Senior BA, et al. *Septal deviation and nasal resistance: an investigation using virtual surgery and computational fluid dynamics.* Am J Rhinol Allergy 2010;24:e46-53.
22. Guo Y, Zhang Y, Chen G et al. *[A computational fluid dynamics study of inner flow through nasal cavity with unilateral hypertrophic inferior turbinate].* Lin Chung Er Bi Yan Hou Tou Jing Wai Ke Za Zhi 2009;23:773-7.
23. Lee HP, Garlapati RR, Chong VF, et al. *Effects of septal perforation on nasal airflow: computer simulation study.* J Laryngol Otol 2010;124:48-54.
24. Lee HP, Poh HJ, Chong FH, et al. *Changes of airflow pattern in inferior turbinate hypertrophy: a computational fluid dynamics model.* Am J Rhinol Allergy 2009;23:153-8.
25. Liu T, Han D, Wang J et al. *Effects of septal deviation on the airflow characteristics: using computational fluid dynamics models.* Acta Otolaryngol 2012;132:290-8.
26. Sun XZ, Tang YY, Liu YX, et al. *[Analysis of the character of self-adaptation of nasal structure in patients with nasal septum deviation].* Zhonghua Er Bi Yan Hou Tou Jing Wai Ke Za Zhi 2008;43:351-4.
27. Zhu JH, Lee HP, Lim KM, et al. *Inspirational airflow patterns in deviated noses: a numerical study.* Comput Methods Biomech Biomed Engin 2012 Apr 19 [Epub ahead of print].
28. Bockholt U, Mlynski G, Muller W, et al. *Rhinosurgical therapy planning via endonasal airflow simulation.* Comput Aided Surg 2000;5:175-9.

[29] Iwasaki T, Saitoh I, Takemoto Y, et al. *Improvement of nasal airway ventilation after rapid maxillary expansion evaluated with computational fluid dynamics.* Am J Orthod Dentofacial Orthop 2012;141:269-78.

[30] Ozlugedik S, Nakiboglu G, Sert C, et al. *Numerical study of the aerodynamic effects of septoplasty and partial lateral turbinectomy.* Laryngoscope 2008;118:330-4.

[31] Wexler D, Segal R, and Kimbell J. *Aerodynamic effects of inferior turbinate reduction: computational fluid dynamics simulation.* Arch Otolaryngol Head Neck Surg 2005;131:1102-7.

[32] Xiong G, Zhan J, Zuo K, et al. *Numerical flow simulation in the post-endoscopic sinus surgery nasal cavity.* Med Biol Eng Comput 2008;46:1161-7.

[33] Chen XB, Lee HP, Chong VF, et al. *Drug delivery in the nasal cavity after functional endoscopic sinus surgery: a computational fluid dynamics study.* J Laryngol Otol 2012;126:487-94.

[34] Frank DO, Kimbell JS, Cannon D, et al. *Deviated nasal septum hinders intranasal sprays: a computer simulation study.* Rhinology 2012;50:311-8.

[35] Frank DO, Kimbell JS, Cannon D, et al. *Computed intranasal spray penetration: comparisons before and after nasal surgery.* Int Forum Allergy Rhinol 2013;3:48-55.

[36] Garlapati RR, Lee HP, Chong FH, et al. *Indicators for the correct usage of intranasal medications: A computational fluid dynamics study.* Laryngoscope 2009;119:1975-82.

[37] Bailie N, Hanna B, Watterson J, et al. *A model of airflow in the nasal cavities: Implications for nasal air conditioning and epistaxis.* Am J Rhinol Allergy 2009;23:244-9.

[38] Pless D, Keck T, Wiesmiller K, et al. *Numerical simulation of air temperature and airflow patterns in the human nose during expiration.* Clin Otolaryngol Allied Sci 2004;29:642-7.

[39] Sommer F, Kroger R, Lindemann J. *Numerical simulation of humidification and heating during inspiration within an adult nose.* Rhinology 2012;50:157-64.

[40] Ishikawa S, Nakayama T, Watanabe M, et al. *Flow mechanisms in the human olfactory groove: numerical simulation of nasal physiological respiration during inspiration, expiration, and sniffing.* Arch Otolaryngol Head Neck Surg 2009;135:156-62.

[41] Wexler D, Segal R, Kimbell J. *Aerodynamic effects of inferior turbinate reduction: computational fluid dynamics simulation.* Arch Otolaryngol Head Neck Surg 2005;131:1102-7.

[42] Sung SJ, Jeong SJ, Yu YS, et al. *Customized three-dimensional computational fluid dynamics simulation of the upper airway of obstructive sleep apnea.* Angle Orthod 2006;76:791-9.

[43] Xu C, Sin S, McDonough J M et al. *Computational fluid dynamics modeling of the upper airway of children with obstructive sleep apnea syndrome in steady flow.* J Biomech 2006;39:2043-54.

[44] Prinsell JR. *Maxillomandibular advancement surgery for obstructive sleep apnea syndrome.* J Am Dent Assoc 2002;133:1489-97; quiz 1539-40.

[45] Yu CC, Hsiao HD, Lee LC, et al. *Computational fluid dynamic study on obstructive sleep apnea syndrome treated with maxillomandibular advancement.* J Craniofac Surg 2009;20:426-30.

[46] Bachert C, Bousquet J, Canonica GW, et al. *Levocetirizine improves quality of life and reduces costs in long-term management of persistent allergic rhinitis.* J Allergy Clin Immunol 2004;114:838-44.

[47] Canonica GW, Fumagalli F, Guerra L, et al. *Levocetirizine in persistent allergic rhinitis: continuous or on-demand use? A pilot study.* Curr Med Res Opin 2008;24:2829-39.

[48] De Vos C, Bachert C. *Business and science: a partnership for the benefit of allergic patients.* Clinical & Experimental Allergy Reviews 2006;6:25-9.

[49] Eitel G, Freitas R, Lintermann A, et al. *Numerical simulation of nasal cavity flow based on a lattice-boltzmann method.* New Results in Numerical and Experimental Fluid Mechanics VII 2010; p. 513-520.

[50] Adams R, Bischof L. *Seeded region growing.* Pattern Analysis and Machine Intelligence, IEEE Transactions on 1994;16:641-7.

[51] Lorensen WE, Cline HE. *Marching cubes: a high resolution 3D surface construction algorithm.* ACM Siggraph Computer Graphics 1987;21:163-9.

[52] Taubin G, Zhang T, Golub G. *Optimal surface smoothing as filter design.* Computer Vision - ECCV'96 1996; p. 283-292.

[53] Bouzidi M, Firdaouss M, Lallemand P. *Momentum transfer of a Boltzmann-lattice fluid with boundaries.* Physics of Fluids 2001;13:3452.

[54] Finck M, Hänel D, Wlokas I. *Simulation of nasal flow by lattice Boltzmann methods.* Comput Biol Med 2007;37:739-49.

[55] Hebert JR, Nolop K, Lutsky BN. *Once-daily mometasone furoate aqueous nasal spray (Nasonex) in seasonal allergic rhinitis: an active- and placebo-controlled study.* Allergy 1996;51:569-76.

[56] Mandl M, Nolop K, Lutsky BN. *Comparison of once daily mometasone furoate (Nasonex) and fluticasone propionate aqueous nasal sprays for the treatment of perennial rhinitis. 194-079 Study Group.* Ann Allergy Asthma Immunol 1997;79:370-8.

[57] Meltzer EO, Jalowayski AA, Orgel HA, et al. *Subjective and objective assessments in patients with seasonal allergic rhinitis: effects of therapy with mometasone furoate nasal spray.* J Allergy Clin Immunol 1998;102:39-49.

[58] Bernhöft I. *Visualisierung der Verbesserung des nasalen Flows unter Behandlung mit einem nasalen Steroid*. Universität zu Köln: Köln, 2011.

[59] Bachert C. *A review of the efficacy of desloratadine, fexofenadine, and levocetirizine in the treatment of nasal congestion in patients with allergic rhinitis.* Clin Ther 2009;31:921-44.

[60] Klimek L. *Potential of levocetirizine in the relief of nasal congestion.* Int J Clin Pract 2005;59:721-9.

[61] Patou J, De Smedt H, van Cauwenberge P, et al. *Pathophysiology of nasal obstruction and meta-analysis of early and late effects of levocetirizine.* Clin Exp Allergy 2006;36:972-81.

Received: December 1, 2012 - Accepted: December 12, 2012

Address for correspondence: Ralph Mösges, Institute of Medical Statistics, Informatics and Epidemiology (IMSIE), University Hospital of Cologne, 50924 Cologne, Germany. Tel. +49 221 478 3456. Fax +49 221 478 3465. E-mail: ralph@moesges.de